RSC Advances

ROYAL SOCIETY OF CHEMISTRY

PAPER

View Article Online
View Journal | View Issue

Cite this: *RSC Adv.*, 2025, **15**, 14632

Study on the properties and *in vitro* transdermal delivery and cytotoxicity of drug-active ionic liquids with matrine as the cation†

Meng Ting,[ab] Liangliang Hu,[a] Yifan Wang,[a] Shijie Wei,*[b] Shaolong He,[b] Qing Huang*[a] and Zhizhong Wang *[a]

Received 18th November 2024
Accepted 8th April 2025

DOI: 10.1039/d4ra08188a

rsc.li/rsc-advances

Combining ionic liquids with active pharmaceutical ingredients (API-ILs) is an ideal strategy to improve the biopharmaceutical properties of APIs while preserving their efficacy. The appropriate selection of anions and cations for the formation of ILs eliminates the problems of solid drugs and retains the core ideal characteristics of the ionic liquid material state. In this study, API-ILs were prepared using matrine (Mat) as a cation and non-steroidal anti-inflammatory drugs (NSAIDs) as anions to improve the undesirable properties of NSAIDs and prepare API-ILs with dual functions. Mass spectrometry showed that the drug molecules exist as anions and cations in the ionic liquid. Infrared, nuclear magnetic and computer simulations demonstrated that Mat-NSAID interactions were mediated by hydrogen bonds, ionic bonds and van der Waals forces. Evaluation of physicochemical properties shows that ILs exhibited better solubility, where the solubilities of loxoprofen and diclofenac were 287 and 220 times higher, respectively, than that of the bulk drug. In addition, cytotoxicity tests were performed prior to *in vitro* skin penetration studies. The accumulation of diclofenac and loxoprofen ionic liquids in the skin was better than that of the corresponding APIs. These results suggest that the utilization of ionic liquids is a simple and effective strategy to improve the undesirable properties of drugs, and the effective selection of cations and anions is essential to regulate the pharmaceutical properties of drugs.

Introduction

Ionic liquids are molten salts composed of anions and cations with a melting point of less than 100 °C at room temperature. They have the characteristics of low volatility, high stability, high conductivity and non-flammability. The cationic ions of ionic liquids are usually very large in volume, and their structure is highly asymmetrical and cannot be tightly packed in the crystal space. The cations can vibrate, transmit and rotate; thus, the crystal structure is completely destroyed, the inter-ion force becomes weaker, the crystal lattice can become smaller, the melting point is reduced, and the ionic compounds can be liquid at room temperature. The preparation method for ionic liquids is simple, including direct synthesis, two-step synthesis and other synthesis methods.[1,2] According to the development history of ionic liquids, they can be divided into three generations. At present, third-generation ionic liquids with drug activity and certain functions are mostly studied.[3,4] API-ILs, a new drug delivery system formed by an API and its corresponding counter-ion or two different APIs, can effectively improve the solubility, stability and permeability of drugs and better play the therapeutic role of drugs.[5] According to the different formation mechanisms, API-ILs mainly has three forms (Fig. 1): (1) for ionic APIs, the ionic bond is combined with a counter-ion; (2) neutral APIs form ionic prodrugs through covalent bonds and then combine with counter-ions; (3) for two different APIs, the above two ways are combined to form a dual-function API-IL system.[6] Compared with the parent API, the formation of API-ILs can increase the solubility of the API, promote permeability, liquefy the solid drug, improve the polymorphic transformation of the solid drug, and thus improve bioavailability.[5]

Efficient design and selection of ions can improve API-ILs synergies. Atiye *et al.*[8] synthesized ionic liquids of active pharmaceutical ingredients with dual biological functions of analgesia and anti-inflammatory properties by combining cations of lidocaine with anions of hydrophobic non-steroidal anti-inflammatory drugs. Matrine (Mat) was selected as a cation in this study. It is a water-soluble alkaloid extracted and isolated from the dried roots, fruits, and other parts of the leguminous plant *Sophora flavescens* (Fig. 2a). It has a variety of pharmacological activities, such as anti-inflammatory, anti-tumor, antiviral, liver protection, anti-arrhythmia, *etc.*[9] Wang *et al.* found

[a]*School of Pharmacy, Ningxia Medical University, Yinchuan, Ningxia, P. R. China. E-mail: 20040024@nxmu.edu.cn; wangzzsc@163.com*

[b]*Department of Pharmacy, General Hospital, Ningxia Medical University, Yinchuan 750004, China. E-mail: nxwsj1978@163.com*

† Electronic supplementary information (ESI) available. See DOI: https://doi.org/10.1039/d4ra08188a

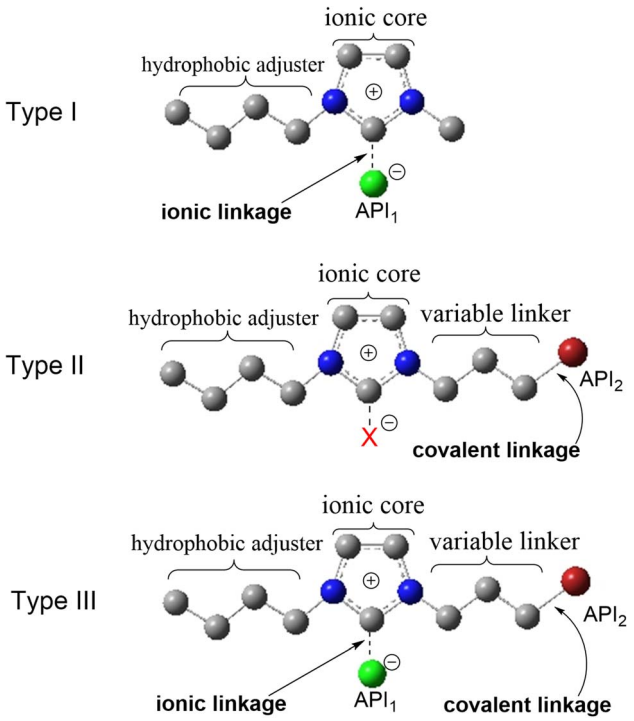

Fig. 1 Three API-ILs with different formation mechanisms.[7]

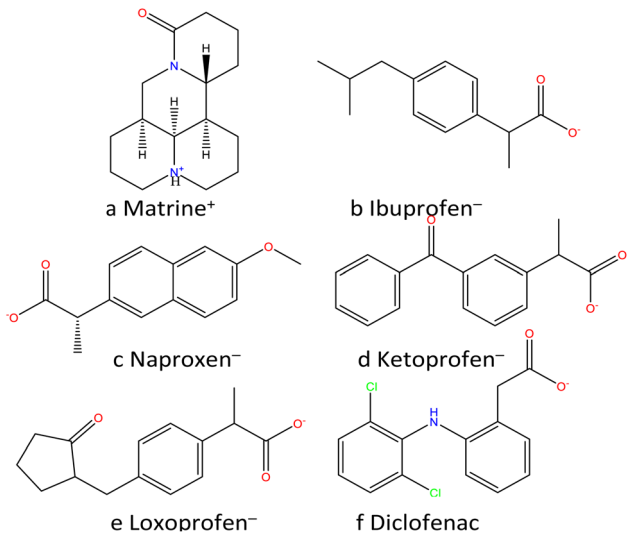

Fig. 2 Structure of counter-ionic matrine and its ionic APIs ibuprofen, naproxen, ketoprofen, loxoprofen, and diclofenac.

that the synergistic effect between bioacive salts that made of natural products Mat cation and phenolic acid anions (*e.g.* [Mat][Syr] and [Mat][Van] with melting points of 91.1 °C and 69.2 °C, respectively), which significantly improve the solubility, antibacterial, anticancer, anti-inflammatory, *etc.* This suggested that salt formation with Mat is a sustainable and effective method for enhancing the pharmaceutical applicability of phenolic acids.[10]

Non-steroidal anti-inflammatory drugs (NSAIDs) belong to Class II drugs of the Biopharmaceutical classification system (BCS) and are characterized by low solubility and high permeability. However, their low solubility limits their bioavailability. For example, aspirin is only slightly soluble in water (100 mL, 0.33 g).[11] Other NSAIDs such as ibuprofen, naproxen, ketoprofen are almost insoluble in water. The solubility and dissolution rate of drugs directly affect their absorption and bioavailability.[12] Consequently, improving the solubility of insoluble drugs is essential to improve their bioavailability.

In this study, API-ILs were prepared from matrine (Mat) as a cation and non-steroidal anti-inflammatory drugs (NSAIDs, Fig. 2) as anions to improve the undesirable properties of NSAIDs and to prepare API-ILs with dual functions. The prepared API-ILs were characterized by the spectrum. Mass spectrometry (MS) verified the purity and formation of ILs. Infrared spectroscopy (IR), nuclear magnetic resonance (NMR) and computer simulations demonstrated that Mat–NSAIDs interactions were mediated by hydrogen bonds and van der Waals forces. Its physicochemical properties were evaluated, and it exhibited better solubility. In addition, *in vitro* skin penetration and cytotoxicity studies were performed.

Experimental

Materials

Unless otherwise noted, all reagents and materials used were obtained from commercial suppliers and have not been additional purified. Ibuprofen (98% purity) and matrine (AR) were purchased from Chengdu Yuannuo tiancheng Technology Co., Ltd. Naproxen (98.5% purity), 2-(2,6-dichlorophenylamino) phenylacetic acid (diclofenac, 98% purity), 2-((4-(2-oxycycloamyl)methyl)phenyl)propionic acid (loxoprofen, 97% purity), and 2-(3-benzoylphenyl)propionic acid (ketoprofen, 99% purity) were provided by Energy Chemical Anhui Zesheng Technology Co., Ltd. *N*-Octanol (AR) was purchased from Yantai Shuangshuang Chemical Co., Ltd. Anhydrous ethanol and sodium hydroxide (granule) (AR) were purchased from Tianjin Damao Chemical Reagent Factory. Phosphate buffered saline (PBS), 10× pH 7.4 was purchased from Wuhan Servicebio Technology Co., Ltd. (Wuhan, Hubei, China). Potassium dihydrogen phosphate (AR) was purchased from Shanghai Guangnuo Chemical Technology Co., Ltd. Formic acid is LC/MS grade, product of Czech Republic, which was supplied by Yinchuan Weiboxin Biological Technology Co., Ltd (Ningxia, China). Ammonium formate was analytically pure and supplied by Laboratories, Inc. (50 Frontage Road Andover, USA; Tianjin Kaixin Chemical Industry Co., Ltd.) HPLC graded methanol (≥99.9%) was supplied by Yinchuan Weiboxin Biological Technology Co., Ltd (Ningxia, China). Deuterium dimethyl sulfoxide (DMSO-d_6) (99.9% purity, 0.03% v/v TMS) was supplied by Cambridge Isotope.

Preparation of API-ILs

The target ionic liquid was prepared by one-step synthesis. Taking matrine ibuprofen ([Mat][Ibu]) ionic liquid as an

example, the equivalent Mat (248.37 mg, 1 mmol) and Ibu (206.29 mg, 1 mmol) were dissolved in anhydrous ethanol (20 mL), stirred at room temperature for 24 h, concentrated under reduced pressure to remove the solvent, and a clear liquid was finally obtained. The preparation of the other ionic liquids is the same as the above steps. Ibuprofen ionic liquid ([Mat][Ibu]) and naproxen ionic liquid ([Mat][Nap]) were light yellow transparent liquids. Loxoprofen ionic liquid ([Mat][Lox]), diclofenac ionic liquid ([Mat][Dic]), and ketoprofen ionic liquid ([Mat][Ket]) are yellow transparent liquids.

Mass spectrum (MS)

Direct infusion electrospray ionization mass spectrometry (ESI-MS) on the API 4000 quadrupole tandem mass spectrometer (Aibo talent Co., Ltd., USA) was used to accurately measure the quality and detect the purity of the ILs. The ILs sample was dissolved in methanol. Cations and anions were analysed in positive ion and negative ion modes, respectively.

Nuclear magnetic resonance spectrum (NMR)

NMR measurements were performed on a Bruker Avance III 400 spectrometer (Bruker BioSpin Co. Ltd, Germany) operating at 400 MHz, and data processing was performed using MestReNova 14 software.

Infrared spectrum (IR)

Infrared spectroscopy was measured using the Tensor 27 Fourier Infrared spectrometer (Bruker, Germany) and the spectrum was obtained by 64 scans in the range of 4000–400 cm^{-1}. The resolution of the instrument is 8 cm^{-1}.

Computational methodology

The APIs and API-ILs were simulated using Gaussian 16 software, Multiwfn[13] and VMD[14] programs. First, the single molecule of five NSAIDs and Mat and the combination of two molecules of five API-ILs were calculated to optimize the ground state molecular structure and frequency based on the Custom/6-31G(d)/m062x method (Gaussian 16). Multiwfn and VMD programs were further used to map the intermolecular van der Waals force penetration.

Detection oil–water partition coefficient

The *n*-octanol–water oil–water partition coefficient was determined by the shaker method and ultraviolet spectrophotometry.[15] First, a standard curve was prepared. Twelve mg of API (Mat, Ibu, Nap, Ket, Lox, and Dic) was precisely measured and placed in a 25 mL volumetric bottle, diluted to the scale with PBS pH 7.4 (ref. 16) or aqueous ethanol solution, and scanned at the full wavelength of 200–800 nm to determine the maximum absorption wavelength (λ_{max}) of the API.

The mother liquor (*e.g.*, 0.09 mL, 0.1 mL, 0.2 mL, 0.3 mL, and 0.4 mL of Mat) was accurately pipetted in a 10 mL volumetric flask and diluted to the scale with buffer. Standard solutions were prepared at concentrations (C) of 4.28 μg mL^{-1}, 4.76 μg mL^{-1}, 9.52 μg mL^{-1}, 14.28 μg mL^{-1} and 19.04 μg mL^{-1}, and the absorbance (A) was measured at λ_{max}. A and C were linearly regressed, and the standard curve was plotted.

PBS pH 7.4 was pre-saturated with *n*-octanol before the experiment. Mat and five kinds of API-ILs were precisely weighed in a 25 mL volumetric bottle and diluted to the scale with a saturated solution of *n*-octanol to prepare the mother liquor. Five mL was removed from the mother liquor, added into a vial and an equal amount of water saturated *n*-octanol solution was added. For non-steroidal anti-inflammatory drugs that are insoluble in water (*e.g.*, ibuprofen), the substance was accurately weighed in a 25 mL volumetric flask, diluted with saturated *n*-octanol solution to the scale line, and its concentration was set as C_0. Five mL of the solution was dispensed into a vial and the same amount of *n*-octanol saturated aqueous solution was added. The vial was shaken in an oscillator at 37 °C for 24 h. After shaking, the sample was centrifuged at 8000 rpm for 10 minutes to ensure complete phase separation. An appropriate amount of the lower aqueous solution was placed in 10 mL and diluted to the scale with PBS pH 7.4. The absorbance was determined as A_W, its concentration (C_W) was obtained according to the standard curve, and the original concentration C was obtained according to the dilution ratio. Then, the oil–water partition coefficient is determined by $K = (C_0 - C)/C$. The measurement of the oil–water partition coefficient is always repeated three times.

Determination of equilibrium solubility

The saturation solubility of APIs and API-ILs was determined in PBS pH 7.4.[17] In the case of ibuprofen, excess Ibu, Mat, IL([Mat][Ibu]) were added into a vial containing 10 mL of buffer and sealed. The vial was placed in a thermo-statically controlled shaking bath and stirred at 100 rpm and 37 °C. After 24 h, the vial was removed, filtered, and the concentrations of Mat and NSAIDs were analysed by spectrophotometry.

Cytotoxicity test

Human normal hepatocytes L02 (purchased from Sebiocom Shanghai Biotechnology Co., Ltd.) were cultured in medium 1640 (Wuhan Seville Biotechnology Co., Ltd.), supplemented with 10% fetal bovine serum (Wuhan Seville Biotechnology Co., Ltd.), and 1% triple antibody (Wuhan Seville Biotechnology Co., Ltd.). The samples to be tested are completely dissolved in medium 1640 and diluted to different concentrations. Log-phase L02 cells are seeded at a density of 1105 cells per well in 96-well plates and incubated at 37 °C for 24 h in a 5% CO_2 atmosphere. The medium in the wells was replaced with the sample solution, and a neat medium was used as a control. After 24 h of incubation, 100 μL of CCK-8 solution was added to each well for 1 h, and the optical density (OD) was measured at 450 nm using a Bio-Tek Gen 5 microplate reader. Eqn (1) was used to calculate the cytostatic rate (%) cell viability of each group according to the following formula:

$$\text{Cell inhibition (\%)} = (A_{control} - A_{sample})/(A_{control} - A_{blank}) \quad (1)$$

$A_{control}$, A_{sample} and A_{blank} are the OD values of the control, sample solution and cell-free wells. Medium 1640 with 1% v/v DMSO was used to solubilize ILs-[Mat][Ibu], ILs-[Mat][Nap], ILs-[Mat][Lox], ILs-[Mat][Dic], ILs-[Mat][Ket] and the physical mixture. The cytotoxicity of API-ILs and its physical mixture to L02 cells was studied at 0.2 mg mL^{-1}, 0.4 mg mL^{-1}, 0.6 mg mL^{-1}, 0.8 mg mL^{-1}, 1 mg mL^{-1} and 2 mg mL^{-1} for 24 h using the CCK-8 method. The experiment was performed in triplicate, and the sample data was analysed using GraphPad Prism 8.0 to determine the IC_{50} value.

Skin permeability study *in vitro*

A Franz diffusion cell (C-0810, Huanghai, Shanghai Yuyan Scientific Instrument Co., Ltd.) was used to study skin permeability *in vitro*.[18–22] The effective mass transfer area was 2 cm^2, the recipient chamber volume was 8 mL, and the donor chamber volume was 2 mL. The recipient cavity was filled with PBS pH 7.4 buffer, and the contents were stirred with a magnetic stirring rod at a rotational speed of 300 rpm. In each diffusion unit, a constant temperature of 37.0 ± 0.1 °C was maintained. The equal molar amount of the API and the API-ILs were dissolved in 2 mL 70% ethanol and added to the donor chamber. The concentration of the solution used is 0.01–0.03 g mL^{-1}. Fresh pig skin (purchased from Huilang Biao Beijing Biotechnology Co., Ltd.) was washed several times in PBS pH 7.4 buffer before *in vitro* penetration tests. The 1 mm thick skin was cut into a circular sample with a radius of 0.8 cm and stored at −80 °C with plastic wrap. On the day of the experiment, the skin samples were slowly thawed at room temperature for 30 minutes, then hydrated with PBS solution. The cut skin was placed between the donor chamber and the recipient chamber in the Franz diffusion cell so that the side of the cuticle was facing the donor chamber. The experiment was carried out for 24 h, and 0.5 mL samples were taken after stirring for 0.5 h, 1 h, 2 h, 3 h, 4 h, 5 h, 8 h and 24 h. At each sample extraction point, the chamber was refilled with 0.5 mL of fresh buffer solution. The concentration of the sample to be measured in the collected receptor phase was determined by high performance liquid chromatography, and the cumulative permeability Q_s (μg cm^{-2})[23] was calculated, as shown in eqn (2).

$$Q_s = C_{sn} \times V_s/A_s + \sum_{i-1}^{n-1} C_{si} \times S/A_s \quad (2)$$

Q_s is the cumulative amount of drug penetration per unit area (μg cm^{-2}), C_{sn} is the concentration of drug in the receiving body fluid measured over n sampling intervals (μg mL^{-1}), and V_s is the volume of the receptor pool (8 mL). $\sum_{i-1}^{n-1} C_{si}$ is the cumulative concentration of the drug in the receiving solution, S is the sample volume (2 mL), and A_s is the effective diffusion area (0.64 π).

The permeability of the sample to be measured through membrane P (cm s^{-1}) is calculated according to eqn (3).

$$-\ln(1 - 2C_t/C_0) = 2A/V \times P \times t \quad (3)$$

In the formula, C_t is the concentration of the recipient chamber at time t, C_0 is the initial concentration of the donor chamber, A is the effective mass transfer area, and V is the total volume of the solution in the two chambers.[24,25]

According to the derived solution of Fick's diffusion law, the diffusion coefficient D (cm^2 s^{-1}) of the API through the film was determined[26] using eqn (4).

$$D = V_1 \times V_2/(V_1 + V_2) \times h/A \times 1/\ln((C_f - C_i)/(C_f - C_t)) \quad (4)$$

where C_f and C_i are the final and initial concentrations of the receptor chamber, and C_t is the concentration of the receptor chamber at time t. V_1 and V_2 are the volume of the donor and recipient chambers, respectively, and h is the thickness of the membrane.

The concentration of the compound under study was determined 24 h after the experiment, according to a previously described method.[27,28] Skin samples were extracted from Franz cells and rinsed with PBS buffers. After drying at room temperature, the skin samples were weighed, cut into pieces incubated in methanol at 4 °C for 24 h, homogenized and then centrifuged. The concentration of active substance in the supernatant was determined by high performance liquid chromatography. The accumulation of the compound under test in the skin was calculated by dividing the mass of the residue after the penetration study by the mass of the skin sample. The cumulative amount is expressed as the mass of active substance per mass of skin (μg active substance per g).

The concentrations of ibuprofen, ketoprofen, naproxen, diclofenac, loxoprofen and their ionic liquids in the acceptor phase and supernatant were determined using a high-performance liquid chromatography system consisting of the following units: Agilent Model 1100 HPLC instrument, ultraviolet detector (Agilent Corporation, USA), chromatographic column (Phenomenex Synergi 4U Hydro-RP 80A; 150 × 4.6 mm, 4 μm). The mobile phase was methanol-1 mmol L^{-1} ammonium formate (containing 0.1% formic acid) (94/6, v/v). The flow rate was 1.0 mL min^{-1}. The signal was detected at λ_{max} (ibuprofen-220 nm, naproxen-230 nm, ketoprofen-260 nm, loxoprofen-223 nm, diclofenac-276 nm). The temperature was 30 ± 0.1 °C. The sample size was 20 μL, and gradient elution should be ultrasonically treated before use.

Results and discussion

Spectrum

The ESI-MS spectra of API-ILs were initially performed in positive and negative ion modes to determine the molecular form of APIs in ILs (Fig. S1–S6†). In the positive ion mode (Fig. S1†), a molecular ion signal with an m/z of 249.1 appeared, corresponding to the protonated matrine molecule $[M + H]^+$ in the ionic liquid. The m/z signal of 271.1 corresponds to the sodiated Mat molecule $[M + Na]^+$ in the ionic liquid. In the negative ion mode (Fig. S2–S6†), a molecular ion signal with an m/z of 205.2 appeared, corresponding to the deprotonated Ibu molecule $[M–H]^-$ in the ionic liquid [Mat][Ibu]; and other molecule signals with m/z of 229.2, 244.8, 294.4, and 252.8 appear, corresponding

to deprotonated Nap, Lox, Dic and Ket molecules in the relevant ionic liquids. Overall, the above results indicated that the active pharmaceutical ingredient molecules exist in the ionic liquid in the form of anions and cations. Additionally, the ionic liquid prepared by the one-step synthesis method of the present invention has a molar ratio of 1 : 1 for the feedstock. In the hydrogen spectrum, the carboxyl active hydrogen of NSAID in the ionic liquid disappeared, and a quaternary ammonium hydrogen signal appeared at δ4.5. Therefore, the two molecules in the ionic liquid theoretically exist in the form of ions at a molar ratio of 1 : 1.

Next, nuclear magnetic resonance spectroscopy, infrared spectroscopy and computer simulation were used to explore the interaction between Mat and NSAIDs in ILs. For APIs with carboxyl function, the following peaks are observed: 3422 cm^{-1}, 2954 cm^{-1} and 1709 cm^{-1} (Ibu), 3426 cm^{-1}, 3253 cm^{-1} and 1723 cm^{-1} (Nap), and 3437 cm^{-1}, 1733 cm^{-1} (Lox). Typical O–H and C=O stretching vibrations were observed at 3437 cm^{-1}, 2884 cm^{-1}, and 1693 cm^{-1} for Dic and 3434 cm^{-1}, 2932 cm^{-1}, and 1695 cm^{-1} for Ket. In the infrared spectrum of API-ILs, the stretching vibration peak of –OH in free acid –COOH becomes weak or almost disappears, with ILs-Ibu (3422 cm^{-1}), ILs-Nap (3426 cm^{-1}), ILs-Lox (3437 cm^{-1}), ILs-Dic (3437 cm^{-1}); For ILs-Ket, the stretching vibration peak of –OH in –COOH changes from 3434 cm^{-1} to 3428 cm^{-1}, the peak widens and the absorption becomes weaker. At the same time, there are obvious $-CO_2^-$ symmetric stretching vibration (V_{sym}) and asymmetric stretching vibration peaks (V_{asym}) in the infrared spectrum of API-ILs. For example, the V_{sym} (CO_2^-) and V_{asym} (CO_2^-) of ILs-Ibu are 1341 cm^{-1} and 1597 cm^{-1}, respectively. The V_{sym} (CO_2^-) and V_{asym} (CO_2^-) of ILs-Nap were 1385 cm^{-1} and 1599 cm^{-1}, respectively. The V_{sym} (CO_2^-) and V_{asym} (CO_2^-) values of ILs-Lox were 1341 cm^{-1} and 1594 cm^{-1}, respectively. The V_{sym} (CO_2^-) and V_{asym} (CO_2^-) of ILs-Dic were 1344 cm^{-1} and 1579 cm^{-1}, respectively. The V_{sym} (CO_2^-) and V_{asym} (CO_2^-) of ILs-Ket were 1322 cm^{-1} and 1596 cm^{-1}, respectively. In addition, the five ionic liquids showed significant $V(N–H^+)$ absorption at 2300–2600 cm^{-1}, while Mat showed no absorption in this range, indicating proton transfer between free NSAIDs and Mat. The infrared spectrum diagram of the PM is the superposition of the infrared spectra of the corresponding two substances (Fig. S7–S11†).

There were significant active hydrogen signals in the ^1H NMR of free acid, including Ibu (δ = 12.27 ppm), Nap (δ = 12.35 ppm), Lox (δ = 12.28 ppm), Dic (δ = 12.74 ppm) and Ket (δ = 12.49 ppm). The active hydrogen signal disappeared in API-ILs, and the remaining peaks did not change significantly (Fig. S12–S27†). In ^{13}C NMR, there is an obvious change of chemical shift[3,29,30] (ESI Material, Fig. S28–S38†). In addition, The APIs and API-ILs were simulated using Gaussian 16 software, Multiwfn and VMD programs to plot the intermolecular van der Waals force penetration map (Fig. 3). In the diagram, translucent blue represents the electron-sucking region and translucent red represents the electron-giving region. The red atoms in the molecular skeleton are oxygen, the blue atoms are nitrogen, and the cyan atoms are carbon, the larger cyan atoms in Fig. 3(C) are chlorine atoms and the white atoms are hydrogen. These results indicated that there are hydrogen bonds, ionic bonds and van der Waals force interactions between Mat and NSAIDs in ILs.

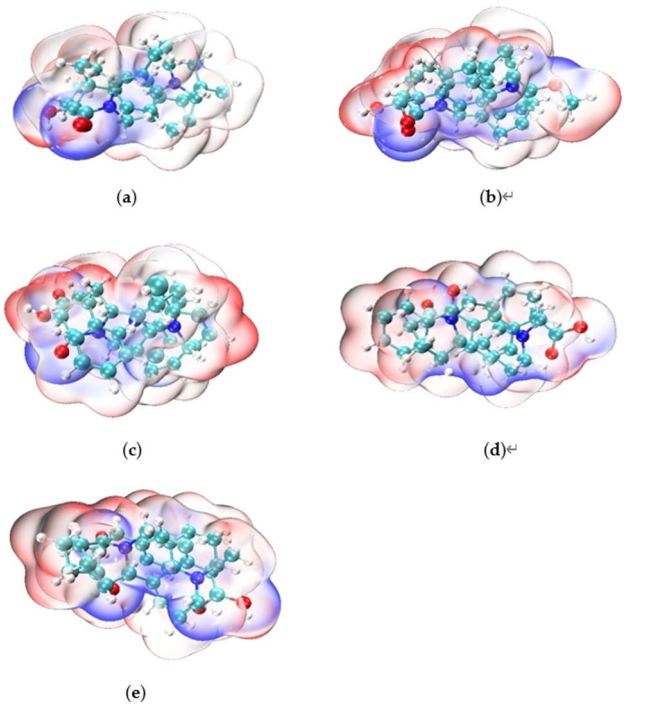

Fig. 3 Intermolecular van der Waals force penetration diagram: (a) Mat and Ibu; (b) Mat and Nap; (c) Mat and Dic; (d) Mat and Ket; (e) Mat and Lox.

API-ILs solubility

API-ILs mother liquor was prepared at 480 μg mL^{-1}, and the specific operation was shown in 3.2.5 (3). The UV absorbance A value was measured at λ_{max}, and the linear regression of the mass molar concentration with absorbance was performed. The standard curves are shown in Table 1.

The solubility of a drug affects its absorption and efficacy, and poor solubility can also cause toxic side effects in application. Therefore, the study of drug solubility is of great significance in the process of drug development.[29] In this study, the shaking bottle method was used to measure the 24 h equilibrium solubility of API and API-ILs in PBS pH 7.4 (Fig. 4). The solubility of API-ILs is significantly higher than that of APIs (Table S1†). The solubility of NSAIDs in ILs expanded more than

Table 1 Standard curve of APIs in PBS pH 7.4

API	Standard curve	R	λ_{max} (nm)
Mat	$y = 0.037x + 0.068$	0.9989	202
Ibu	$y = 0.048x - 0.0068$	0.9993	222
Nap	$y = 0.312x + 0.0209$	0.9993	230
Lox	$y = 0.0362x + 0.0198$	0.9987	223
Dic	$y = 0.0424x - 0.0883$	0.9904	276
Ket	$y = 0.0662x + 0.0019$	0.9989	260

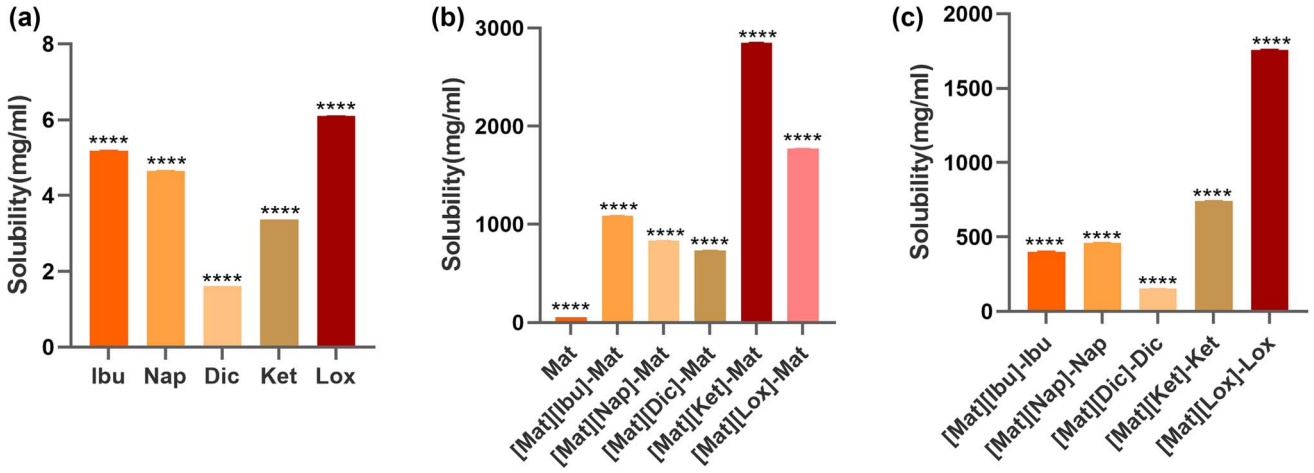

Fig. 4 24 h equilibrium solubility of API and API-ILS in PBS at pH 7.4 (****: significant differences in solubility between APIs and ILS, $P < 0.001$).

with Mat. For example, the solubility of Ibu in [Mat][Ibu] was 78 times larger than that of the API, and the solubility of Mat in [Mat][Ibu] was 20 times larger than that of the API. The reason for this difference may be that ILs are liquid salts, the solubility obviously increases due to the existence of ionic bond after forming ionic liquid, and Mat has better solubility, while there are hydrophobic groups in NSAID molecules, which have a lower solubility in water.[31]

Oil–water distribution coefficient

Drug metabolism is related to the transport distribution of APIs and their affinity with cell membranes, which is a key factor affecting drug bioavailability. However, the distribution coefficient of drugs in the body is difficult to determine. The researchers used the octanol–water partition coefficient as a simplified model to simulate the blood/lipid membrane partition. It has become an important tool for understanding the tendency of chemicals to cross biofilms.[29] As mentioned above, the *n*-octanol–water partition coefficients of APIs and API-ILs were determined by the shaker method (Table 2). From the results of saturation solubility, the oil–water distribution coefficient of NSAIDs is predicted to decrease after the formation of ILs. Contrary to expectations, the increase in the solubility of NSAIDs in the form of ILs is not accompanied by a decrease in the oil–water distribution coefficient, which is the same as the literature.[32] In addition, the oil–water distribution coefficient of Mat varies in different ionic liquids. This indicated that different anions have different effects on the properties of ionic liquids.

Table 2 Oil–water partition coefficient of pure APIs and API-ILs at 37 °C

Samples		Oil–water partition coefficient (K)
Pure APIs	Mat	0.50
	Ibu	0.68
	Nap	0.16
	Lox	−0.81
	Dic	1.16
API-ILs	Ket	0.043
	[Mat][Ibu]-Mat	0.54
	[Mat][Ibu]-Ibu	1.19
	[Mat][Nap]-Mat	0.39
	[Mat][Nap]-Nap	0.92
	[Mat][Lox]-Mat	0.27
	[Mat][Lox]-Lox	0.52
	[Mat][Dic]-Mat	1.22
	[Mat][Dic]-Dic	1.95
	[Mat][Ket]-Mat	0.48
	[Mat][Ket]-Ket	1.14

Cytotoxicity test

Cytotoxicity was assessed by the CCK-8 assay. The effects of five APIs and API-ILs on L02 cells at concentrations of 0.2–2 mg mL^{-1} were studied using PM as the positive control group. In Fig. 5, the IC_{50} value of the API on L02 cells was between 0.2–1.0 mg mL^{-1}. The choice of anion can change the toxicity of API-ILs. The toxicity of Ket and Dic ionic liquid is reduced, with IC_{50} values of about 2 mg mL^{-1} and 0.6 mg mL^{-1}, respectively (API is 0.2–0.4 mg mL^{-1}) (Fig. 6). Ibu, Nap and Lox ionic liquids showed increased toxicity, with a cell median inhibition concentration of about 0.6 mg mL^{-1} (Ibu is 0.6–0.8 mg mL^{-1}), 0.4 mg mL^{-1} (Nap is about 0.6 mg mL^{-1}) and 0.4 mg mL^{-1} (Lox is between 0.6–0.8 mg mL^{-1}).

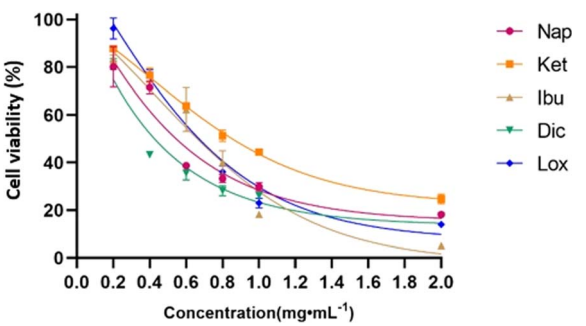

Fig. 5 Cytotoxicity of APIs ($n = 3$, $\bar{X} \pm S$).

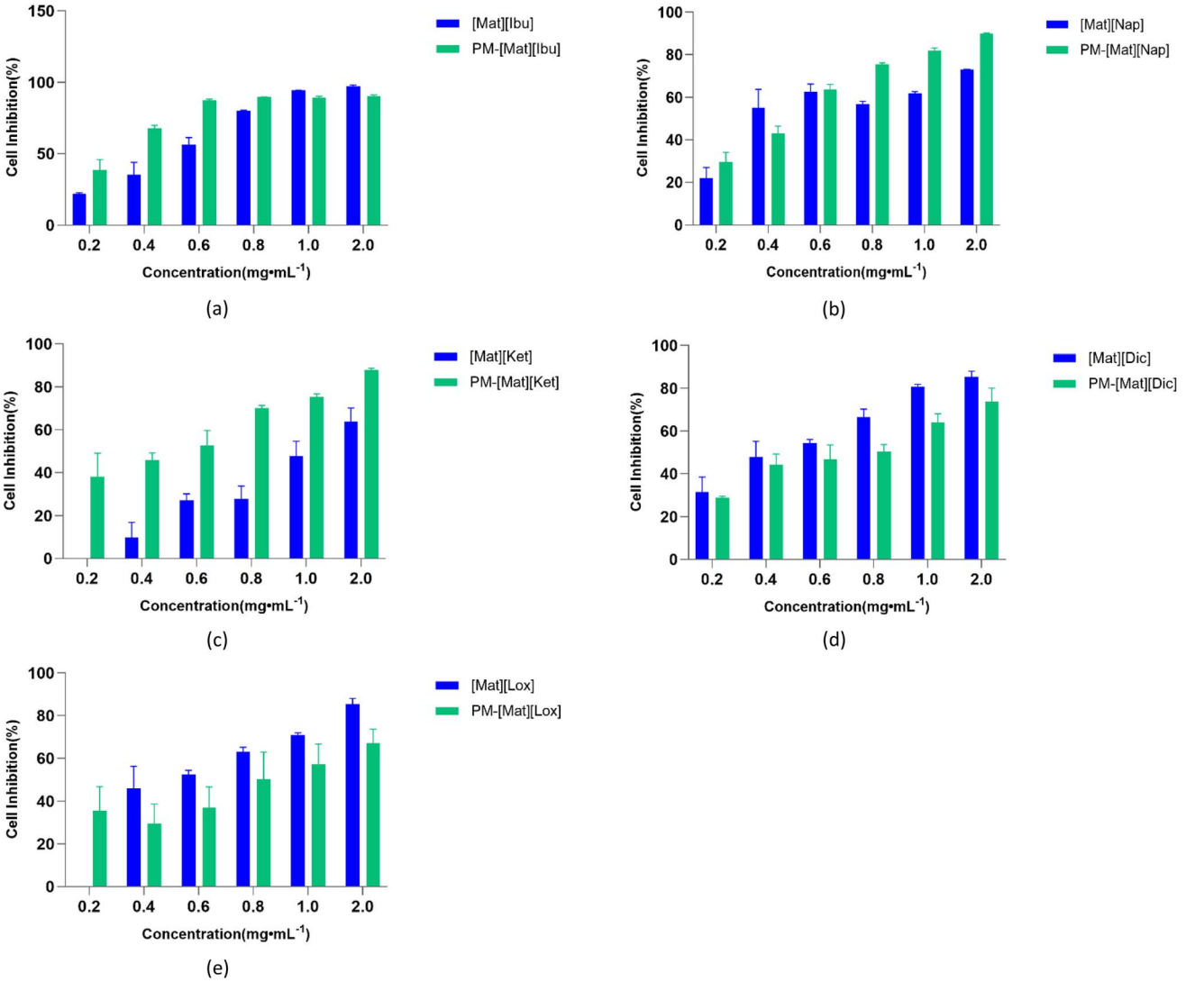

Fig. 6 Cytotoxicity of API-ILs and their physical mixture ($n = 3$, $\bar{X} \pm S$).

In addition, API-ILs and its PM showed dose-dependent cytotoxicity to L02 cells. When the compounds were treated for 24 h, overall cell survival in each group indicated that ketoprofen ionic liquid ([Mat][Ket]) and naproxen ionic liquid ([Mat][Nap]) were less toxic than their physical mixtures, while [Mat][Dic], [Mat][Ibu] and [Mat][Lox] ionic liquids were more toxic than their physical mixtures. The ILs have the effect of changing the cell arrangement and promoting transdermal penetration. Therefore, it is speculated that the toxicity of API-ILs may be related to the permeability of cell membrane and the change of the oil–water distribution coefficient.

Skin permeability *in vitro*

When NSAIDs form ionic liquids, their permeability and diffusion may change. In this section, fresh pig skin was used for a skin penetration study, which is highly comparable to human skin due to its similar histological and physiological properties.[33–36] A Franz diffusion cell was used to compare the permeability of NSAIDs with the corresponding API-ILs. The donor phase was an ethanol solution with a mass concentration of 0.01–0.03 g mL^{-1} (70%, v/v), and the acceptor phase was PBS pH 7.4. The permeation curve of each NSAID with ionic liquid at a specified time point is shown in Fig. 7, and the final cumulative amount (Q_s 24) of a single compound measured after 24 h of permeation is summarized in Table 3. The concentration of ibuprofen was low in 0–8 h, and the final cumulative amount at 24 h was 512.08 μg cm^{-2}. The final cumulative amount of ibuprofen ionic liquid ([Mat][Ibu]) was 144.60 μg cm^{-2}, which was lower than that of the parent drug. Meanwhile, the final accumulations of naproxen ionic liquid (116.15 μg cm^{-2}) and ketoprofen ionic liquid (238.33 μg cm^{-2}) were lower than those of the parent drug (Nap-567.19 μg cm^{-2} and Ket-421.18 μg cm^{-2}). However, the final accumulation of diclofenac ionic liquid (285.21 μg cm^{-2}) and loxoprofen ionic liquid (557.25 μg cm^{-2}) was higher than that of the parent drug (Dic-220.96 μg cm^{-2} and Lox-110.63 μg cm^{-2}). In addition, the accumulation of [Mat][Ibu] and [Mat][Lox] in the skin increased significantly during the transdermal period of 8–24 h (Fig. 7a and e) because

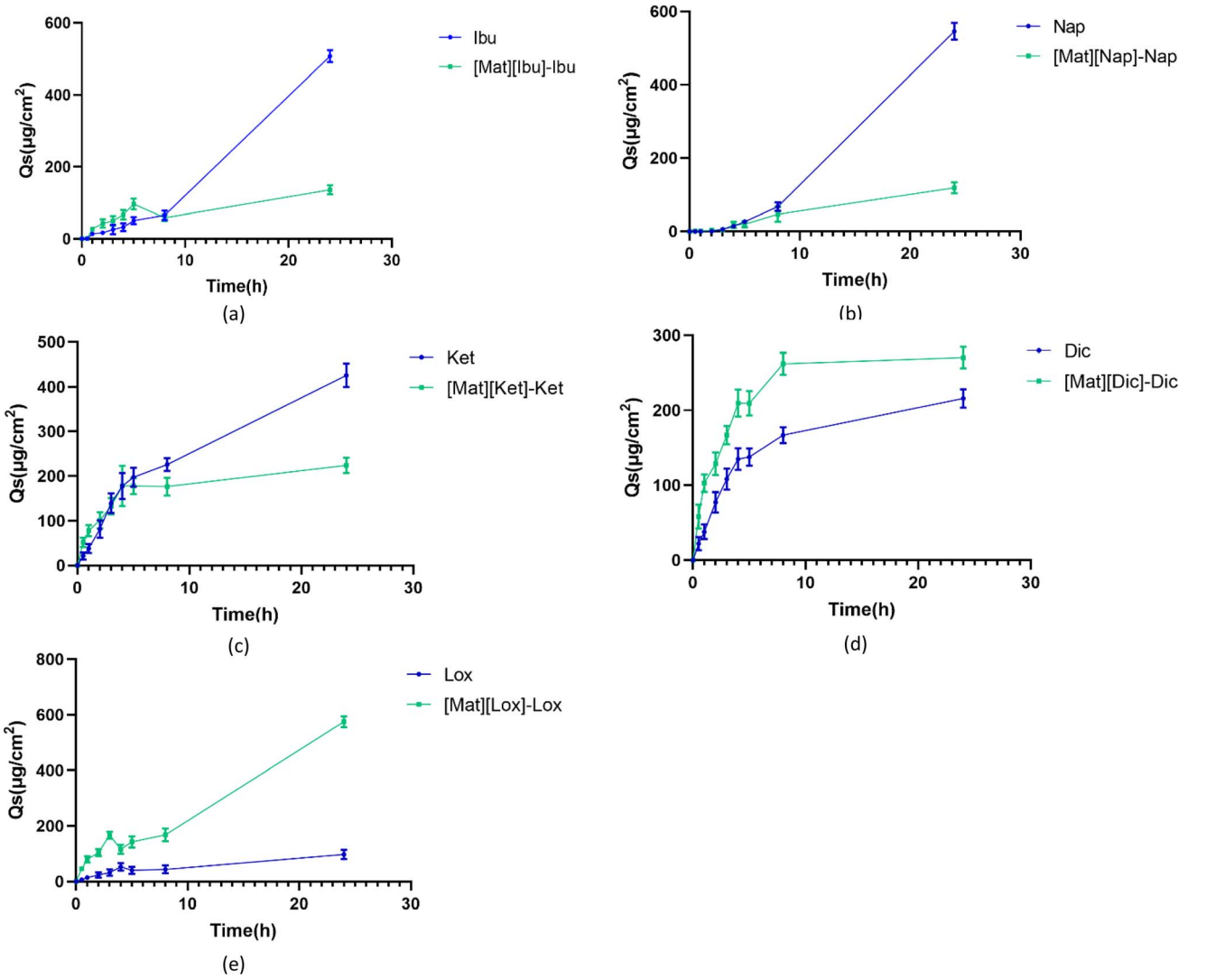

Fig. 7 (a–e) *In vitro* skin permeability of non-steroidal anti-inflammatory drugs and ionic liquids ($n = 3$, $\bar{X} \pm S$).

the ionic liquid can bypass the barrier of the stratum corneum significantly during the transdermal period of 8–24 h (Fig. 7a and e) because the ionic liquid can bypass the barrier of the stratum corneum by destroying the integrity of the skin cells, fluidizing the keratin layer, establishing diffusion channels, and extracting lipid components from the stratum corneum, thus, promoting percutaneous penetration of the drug. Furthermore, an obvious increase in the amount of accumulation in the skin was observed in Ibu and Nap, which may be related to their higher permeability parameter P values.

Through the evaluation of the efficiency of the penetration study, the permeability parameters were determined: diffusion

Table 3 Skin penetration parameters of different non-steroidal anti-inflammatory drugs and ionic liquids ($n = 3$, $\bar{X} \pm S$)

Samples	Cumulant (μg g^{-1})	D (10^{-7} cm^2 s^{-1})	P (10^{-8} cm s^{-1})	Q_s 24 (μg cm^{-2})
Ibu	4885.95 ± 5.13	2.76 ± 0.76	72.70 ± 4.00	512.08 ± 8.54
Nap	3568.92 ± 11.22	1.46 ± 0.13	69.30 ± 6.05	567.19 ± 9.56
Lox	6328.07 ± 8.08	1.83 ± 0.17	9.13 ± 1.07	110.63 ± 3.54
Ket	4776.72 ± 7.16	1.49 ± 0.34	33.50 ± 2.78	421.18 ± 5.66
Dic	2418.55 ± 2.81	5.23 ± 0.29	10.90 ± 3.07	220.96 ± 2.51
[Mat][Ibu]-Ibu	17614.00 ± 10.02	3.65 ± 0.17	6.04 ± 1.00	144.60 ± 6.35
[Mat][Nap]-Nap	2874.14 ± 9.50	5.84 ± 0.22	6.17 ± 1.53	116.15 ± 6.45
[Mat][Lox]-Lox	3637.55 ± 4.56	7.65 ± 0.22	25.80 ± 3.21	557.25 ± 2.95
[Mat][Ket]-Ket	5997.29 ± 5.91	4.53 ± 0.27	0.60 ± 0.51	238.33 ± 11.17
[Mat][Dic]-Dic	7230.31 ± 5.66	19.10 ± 0.70	5.91 ± 1.49	285.21 ± 9.92

coefficient D, permeability P, final accumulation Q_s 24 in the 24 h receptor phase and the accumulation of active substances in the skin (Table 3). The diffusion coefficient reflects the change of the diffusion amount of the drug substance with time. Therefore, the higher the diffusion coefficient, the faster the diffusion rate of the API through the membrane. An increase in the diffusion coefficient was observed when the API was complexed in ionic liquid form. Combined with the solubility results, it can be expected that the diffusion of the API in ionic liquid form will be faster than that of pure API because the higher the solubility, the greater the driving force, and the results are consistent with previous studies.[18]

In addition to the ability to penetrate through the skin, transdermal and topically administered drugs may also accumulate. Therefore, high levels of penetration or accumulation are desirable, depending on the high route of administration chosen. In local delivery systems, low permeability combined with high accumulation is desirable, while the opposite relationship is desirable in transdermal delivery systems.[37–39] Faster and greater penetration and lower skin accumulation are often more advantageous for drug administration in the local system. All of the compounds studied accumulate in the skin. The cumulative quality of ibuprofen, ketoprofen and diclofenac ionic liquids in skin was generally higher than that of unmodified acids. Among these substances, ibuprofen ionic liquid has the highest cumulative value. Contrary to the above results, the cumulative value of naproxen and loxoprofen ionic liquids in the skin was generally lower than that of unmodified acids. In addition, loxoprofen ionic liquid with a lower cumulative mass of skin had the highest cumulative penetration quality after 24 h. In conclusion, ibuprofen, ketoprofen and diclofenac ionic liquids had higher skin accumulation and lower skin penetration. Loxoprofen ionic liquid has higher skin penetration and lower skin accumulation. Naproxen ionic liquid has lower skin accumulation and skin penetration. The above transdermal experiments suggested that ionic liquids formed by different anions have varying degrees of influence on their transdermal performance. This may be related to the structural differences of the anions themselves, changes in the oil–water distribution coefficient, and the intensity of intermolecular interactions.

Conclusions

Five kinds of API-ILs were prepared by a one-step synthesis method. Spectroscopic and molecular simulations of ILs confirmed that Mat and NSAIDs in ionic liquids exist in a 1 : 1 molar ratio of positive and negative ions, and there were interaction forces such as hydrogen bonds, ionic bonds and van der Waals forces. At the same time, the formation of ionic liquid significantly increased the solubility and accumulation of NSAIDs in the skin. In addition, NSAIDs showed different levels of toxicity to human normal hepatocytes (L02) after being converted into ionic liquid, and the choice of anions could change the toxicity of ILs. These results indicated that API-ILs is an effective strategy for modulating the physicochemical and *trans*-dermal properties of NSAIDs. Most importantly, the choice of anions that make up the ionic liquid is critical for modulating the properties of the bulk drug and may produce synergistic therapeutic effects.

Data availability

The data supporting this paper are included in the ESI,† and these data were generated in this study.

Author contributions

Conceptualization, Wang Z.; methodology, Meng T.; software, Meng T.; validation, Wang Z. and Wei S.; formal analysis, Wang Y.; investigation, Hu L.; resources, Huang Q. He S. and Wei S.; data curation, Wang Y.; writing-original draft preparation, Meng T.; writing-review and editing, Wang Z.; visualization, Hu L.; supervision, Wang Z.; project administration, Wang Z. All the authors have read and agreed to the published version of the manuscript.

Conflicts of interest

There are no conflicts to declare.

Acknowledgements

We acknowledge any support given that is not covered in the author contribution or funding section. This may include administrative and technical support or donations in kind (*e.g.*, materials used for experiments). The Key Research & Development Program of Ningxia (No. 2021BEG03102) is gratefully acknowledged.

References

1 Y. Mang, J. P. Tian, and Y. B. Guo, *Introduction to Ionic Liquids*, Chinese High-Tech Enterprises, 2010, (33), pp. 28–29.
2 J. P. Bian, and Q. H. Yang, Advances in synthesis and purification of ionic liquids[J]. *Material Guide*, 2018, 32(11), pp. 1813–1819.
3 X. X. Cao, *Properties of Bifunctional Drug Active Ionic Liquid with Ibuprofen as Anion and its Interaction with Small Biological molecules[D]*, Zhengzhou University, 2021.
4 J. L. Shamshina and R. D. Rogers, Ionic Liquids: New Forms of Active Pharmaceutical Ingredients with Unique, Tunable Properties, *Chem. Rev.*, 2023, **123**(20), 11894–11953.
5 Y. X. Jiang, Q. Jiang, D. Wang, W. T. Zhang, W. He and M. Yang, Application of ionic liquids in drug delivery, *Acta Pharmacol. Sin.*, 2022, **57**(02), 331–342.
6 X. Y. Yang, H. Y. Zhu, Q. Gao, Z. F. Wang, J. He and H. F. Luo, Design of ionic liquids and their application in transdermal drug delivery, *Chin. Pharm. J*, 2023, **54**(05), 665–673.
7 K. S. Egorova, M. M. Seitkalieva, A. V. Posvyatenko, V. N. Khrustalev and V. P. Ananikov, Cytotoxic Activity of Salicylic Acid-Containing Drug Models with Ionic and

Covalent Binding, *ACS Med. Chem. Lett.*, 2015, **6**(11), 1099–1104.

8 A. Abednejad, Polyvinylidene fluoride-Hyaluronic acid wound dressing comprised of ionicliquids for controlled drug delivery and dual therapeutic behavior, *Acta Biomater.*, 2019, **100**, 142–157.

9 D. D. Hu, X. Chen, D. X. Li, H. L. Zhang, Y. W. Duan and Y. Huang, Tranilast-matrine co-amorphous system: Strong intermolecular interactions, improved solubility, and physiochemical stability, *Int. J. Pharm.*, 2023, **25**(635), 122707.

10 M. Wang, Z. Y. Wang, J. C. Zhang, J. B. Zhan, C. Y. Wu, W. Yu, W. H. Fan, J. S. Tang, Q. Q. Zhang and J. H. Zhang, *ACS Sustain. Chem. Eng.*, 2022, **10**(31), 10369–10382.

11 K. Bica, C. Rijksen, M. Nieuwenhuyzen and R. D. Rogers, In search of pure liquid salt forms of aspirin: ionic liquid approaches with acetylsalicylic acid and salicylic acid, *Phys. Chem. Chem. Phys.*, 2010, **12**(8), 2011–2017.

12 J. R. Wang, Study on methods to improve bioavailability of insoluble oral drugs, *Capital Medicine*, 2011, **18**(08), 52–53.

13 L. Tian and C. Feiwu, *J. Comput. Chem.*, 2022, **33**, 580–592.

14 W. Humphrey, A. Dalke and K. Schulten, VMD - Visual Molecular Dynamics, *J. Mol. Graphics*, 1996, **14**(1), 33–38.

15 H. Bando, S. Mohri, F. Yamashita, Y. Takakura and M. Hashida, Effects of skin metabolism on percutaneous penetration of lipophilic drugs, *J. Pharm. Sci.*, 1997, **86**(6), 759–761.

16 *Pharmacopoeia of the People's Republic of China: 2020 Edition. Four-Part*[M], China Medical Science and Technology Press, 2020.

17 J. M. Liang, L. He, Ibuprofen equilibrium solubility and apparent oil–water partition coefficient determination[J], *Straits Pharmacy*, 2016, 28, (03), pp. 66–68.

18 K. Joanna, P. Ossowicz-Rupniewska, A. Nowak, E. Kucharska, Ł. Kucharski, W. Duchnik, L. Struk, A. Klimowicz and E. Januś, Cations of amino acid alkyl esters conjugated with an anion from the group of NSAIDs - as tunable pharmaceutical active ionic liquids, *J. Mol. Liq.*, 2023, **384**, 122200.

19 A. Duarte, A. S. Ferreira, S. Barreiros, E. Cabrita, R. Reis and A. Paiva, A comparison between pure active pharmaceutical ingredients and therapeutic deep eutectic solvents: Solubility and permeability studies, *Eur. J. Pharm. Biopharm.*, 2017, **114**, 296–304.

20 M. Wang, Z. Y. Wang, J. C. Zhang, L. J. Zhang, W. Wang, J. B. Zhan, Y. Liao, C. Y. Wu, W. Yu and J. H. Zhang, A Matrine-Based Supramolecular Ionic Salt that Enhances the Water Solubility, Transdermal Delivery, and Bioactivity of Salicylic Acid, *SSRN Electronic Journal*, 2023, **468**, 143480.

21 H. Tian, Y. J. Wang, S. J. Peng and S. Z. Sun, Transdermal study of resveratrol phospholipid complex in vitro, *West China J. Pharm. Sci.*, 2011, **26**(03), 261–263.

22 E. Janus, P. Ossowicz, J. Klebeko, A. Nowak, W. Duchnik, L. Kucharski and A. Klimowicz, Enhancement of ibuprofen solubility and skin permeation by conjugation with l-valine alkyl esters, *RSC Adv.*, 2020, **10**(13), 7570–7584.

23 T. Q. Liu, L. Hu, B. B. Lu, Y. Y. Bo, Y. Liao, J. B. Zhan, Y. L. Pei, H. Q. Sun, Z. Y. Wang, C. W. Guo and J. H. Zhang, A novel delivery vehicle for copper peptides, *New J. Chem.*, 2023, **47**, 75–83.

24 J. M. Silva, A. R. Duarte, S. Caridade, C. Picart, R. L. Reis and J. F. Mano, Tailored freestanding multilayered membranes based on chitosan and alginate, *Biomacromolecules*, 2014, **15**(10), 3817–3826.

25 H. Y. He, X. Cao and L. J. Lee, Design of a novel hydrogel-based intelligent system for controlled drug release, *J. Control. Release*, 2004, **95**(3), 391–402.

26 P. Ossowicz, J. Klebeko, E. Janus, A. Nowak, W. Duchnik, L. Kucharski and A. Klimowicz, The effect of alcohols as vehicles on the percutaneous absorption and skin retention of ibuprofen modified with L -valine alkyl esters, *RSC Adv.*, 2020, **10**, 41727–41740.

27 E. Janus, P. Ossowicz, J. Klebeko, A. Nowak, W. Duchnik, Ł. Kucharski and A. Klimowicz, Enhancement of ibuprofen solubility and skin permeation by conjugation with L-valine alkyl esters, *RSC Adv.*, 2020, **10**, 7570–7584.

28 A. Haq and B. Michniak-Kohn, Effects of solvents and penetration enhancers on transdermal delivery of thymoquinone: permeability and skin deposition study, *Drug Delivery*, 2018, **25**, 1943–1949.

29 Y. M. Tang, K. Yang, S. Y. Zhao, Q. Q. Chen, L. Qin and B. Qin, Evaluation of Solubility, Physicochemical Properties, and Cytotoxicity of Naproxen-Based Ionic Liquids, *ACS Omega*, 2023, **8**(9), 8332–8340.

30 H. J. Park and M. R. Prausnitz, Lidocaine-ibuprofen ionic liquid for dermal anesthesia, *AIChE J.*, 2015, **61**, 2732–2738.

31 M. Ishikawa and Y. Hashimoto, Improvement in aqueous solubility in small molecule drug discovery programs by disruption of molecular planarity and symmetry, *J. Med. Chem.*, 2011, **54**(6), 1539–1554.

32 S. A. Hassan, S. F. Gad, H. H. M. Abdu-Allah, W. S. Qayed, S. A. AbouElmagd and E. A. Ibrahim, Ionic liquid of ketoprofen-piperine modulates the pharmaceutical and therapeutic characters of ketoprofen, *Int. J. Pharm.*, 2022, **620**, 121724.

33 J. H. Yang, L. Wang, T. Wang, *Determination of equilibrium solubility and apparent oil-water partition coefficient of matrine*, Ningxia Medical University, 2011, vol. 33, pp. 498–499.

34 B. A. Čuříková, K. Procházková, B. Filková, P. Diblíková, J. Svoboda, A. Kováčik, K. Vávrová and J. Zbytovská, Simplified stratum corneum model membranes for studying the effects of permeation enhancers, *Int. J. Pharm.*, 2017, **534**(1–2), 287–296.

35 U. Jacobi, M. Kaiser, R. Toll, S. Mangelsdorf, H. Audring, N. Otberg, W. Sterry and J. Lademann, Porcine ear skin: an *in vitro* model for human skin, *Sking Res. Technol.*, 2007, **13**(1), 19–24.

36 I. M. Khiao, K. C. Richardson, A. Loewa, S. Hedtrich, S. Kaessmeyer and J. Plendl, Histological and functional comparisons of four anatomical regions of porcine skin with human abdominal skin, *Anat., Histol., Embryol.*, 2019, **48**(3), 207–217.

37 E. Touitou, V. M. Meidan and E. Horwitz, Methods for quantitative determination of drug localized in the skin, *J. Controlled Release*, 1998, **56**(1–3), 7–21.
38 H. A. E. Benson, in: Skin Structure, Function, and Permeation, ed. H. A. E. Benson and A. C. Watkinson, *Topical and Transdermal Drug Delivery*, John Wiley & Sons Inc, Hoboken, NJ, USA, 2012, pp. 1–22.
39 R. L. Barkin, Topical Nonsteroidal Anti-Inflammatory Drugs: The Importance of Drug, Delivery, and Therapeutic Outcome, *Am. J. Ther.*, 2015, **22**(5), 388–407.